The Journal of Chemical Physics

Beam investigations of D_2 adsorption on Si(100): On the importance of lattice excitations in the reaction dynamics

Cite as: J. Chem. Phys. **101**, 7082 (1994); https://doi.org/10.1063/1.468419
Submitted: 17 May 1994 • Accepted: 28 June 1994 • Published Online: 31 August 1998

Kurt W. Kolasinski, Winfried Nessler, Karl-Heinz Bornscheuer, et al.

View Online

Export Citation

ARTICLES YOU MAY BE INTERESTED IN

Hydrogen termination of Si(110) surfaces upon wet cleaning revealed by highly resolved scanning tunneling microscopy
Journal of Applied Physics **98**, 103525 (2005); https://doi.org/10.1063/1.2136214

Equilibrium surface hydrogen coverage during silicon epitaxy using SiH_4
Journal of Vacuum Science & Technology A **8**, 2960 (1990); https://doi.org/10.1116/1.576613

In situ investigation of hydrogen interacting with Si(100)
Applied Physics Letters **98**, 211909 (2011); https://doi.org/10.1063/1.3593195

Challenge us.
What are your needs for periodic signal detection?

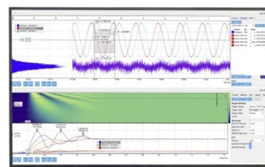

© 1994 American Institute of Physics.

AIP Publishing

Beam investigations of D_2 adsorption on Si(100): On the importance of lattice excitations in the reaction dynamics

Kurt W. Kolasinski, Winfried Nessler, Karl-Heinz Bornscheuer, and Eckart Hasselbrink
Fritz-Haber-Institut der Max-Planck-Gesellschaft, Faradayweg 4-6, D 14195 Berlin, Germany

(Received 17 May 1994; accepted 28 June 1994)

The adsorption of D_2 on Si(100) has been investigated by means of supersonic molecular beam techniques. We have succeeded in measuring the dependence of the molecular D_2 sticking coefficient S on surface temperature T_s and nozzle temperature T_n. The sticking coefficient increases gradually in the range $300 \leq T_n \leq 1040$ K. The influence of increased $v=1$ population has not been deconvoluted from the effects of translational energy alone. The dependence on T_s is more interesting. With an incident translational energy of 65 meV, S rises from a value insignificantly different from the background level to a maximum value of $(1.5 \pm 0.1) \times 10^{-5}$ at $T_s = 630$ K. The decrease in the effective sticking coefficient beyond this T_s is the result of desorption during the experiment. Having established that S increases with both increasing molecular energy and increasing sample temperature, we have demonstrated directly for the first time that the adsorption of molecular hydrogen on Si is activated and that lattice vibrational excitations play an important role in the adsorption process.

I. INTRODUCTION

Hydrogen on silicon is the most in-depth studied of all adsorbate-on-semiconductor systems. While the bulk of this work deals with the interactions in the chemisorbed atomic state, significant attention has recently turned towards attempt to understands the desorption dynamics of molecular hydrogen from Si surfaces. In this work, we report what we believe to be the first reliable results on the adsorption of *molecular* hydrogen on Si single-crystal surfaces.

Sinniah *et al.*[1,2] demonstrated that H_2 desorption from Si(100) follows first-order kinetics. This result was confirmed by Wise *et al.*[3] who also showed that H_2 desorption from Si(111) follows second-order kinetics. Subsequently, Heinz, Höfer, and co-workers[4,5] successfully measured the complete coverage dependencies of the desorption orders and demonstrated systematic deviations from first- and second-order desorption kinetics for Si(100) and Si(111), respectively. These results required a fundamental rethinking of the mechanism of H_2 desorption from Si surfaces.

Wise *et al.*[3] proposed that pairing of H atoms on the dimers inherent to the Si(100)-(2×1) structure lies at the root of the near first-order desorption kinetics. This proposition is supported by the observation of pairing in the scanning tunneling microscopy (STM) images of Boland.[6] The driving force for dimerization stems from the interaction of the dangling bonds found on the unreconstructed Si(100) surface. This interaction has often been referred to as π bonding; however, since the lowest energy state of the dimer appears to be asymmetric (tilted),[7–18] this interaction is better understood as a Peierls distortion (the solid-state analog of the Jahn–Teller effect). An essential lesson to be learned from this interaction is that there are no free-standing dangling bonds on the dimers which make up the clean Si(100)-(2×1) surface. Regardless of the nature of the stabilization, the adsorption of a single H atom destroys the stabilization and it is thus energetically more favorable for a second H atom to adsorb on the same dimer unit rather than on a different dimer which has yet to lose its stabilization energy. Modeling by D'Evelyn and co-workers[19–21] and Höfer, Li, and Heinz[5] have shown that pairing induced by dimer stabilization destruction can adequately describe the desorption kinetics and approximate the STM results.

Finally, Kolasinski, Shane, and Zare (KSZ) using state-specific detection of H_2, HD, and D_2 desorbed from Si(100) (Refs. 22–24) and H_2 from Si(111) (Ref. 25) surfaces demonstrated that the desorbing molecules pass through nearly equivalent transition states on both surfaces. This rules out invoking two significantly different potential energy hypersurfaces, i.e., completely different desorption dynamics, as the cause of the kinetic differences between the two surfaces. Therefore, energetic and structural factors in the chemisorbed phase, namely those leading to pairing on Si(100) and the lack of pairing on Si(111), are responsible for the kinetic differences, while the dynamics of molecular formation and desorption are basically the same for both surfaces. Based on comparisons of the Si(100) and Si(111) monohydride-covered surfaces and mono- and dihydride-covered Si(100) surfaces, KSZ postulated that a dihydride species acts as an intermediate during the desorption process.

Recently the angular distribution of D_2 thermally desorbed from Si(100) has also been measured.[26] It was found that the desorption flux is somewhat peaked in the normal direction ($\cos^n \theta$, with $n=4-5$).

Extensive theoretical analysis has also been carried out. Nachtigall, Janda, and Jordan[27] suggested, based on cluster calculations, that a dihydride species may be involved in the desorption mechanism. A dihydride intermediate has also been found in the calculations of Wu, Ionova, and Carter.[28] Subsequent calculations[28–30] by these two groups and Jing, Lucovsky, and Whitten,[31,32] however, have raised concerns as to whether desorption occurs from a dihydride species on normal dimer units. These groups have found their calculated desorption activation energy for this pathway 3.2–4 eV to be

 0021-9606/94/101(8)/7082/13/$6.00 © 1994 American Institute of Physics

too large compared to the experimentally measured values (≈2.5 eV) and have, therefore, discussed the involvement of defects and diffusion in the desorption mechanism.

Despite the extensive research conducted on the H/Si system, we are still left with several fundamental, unanswered questions: What is the magnitude of the activation barrier to hydrogen adsorption? What is the cause of the low sticking coefficient of H_2 on Si? What is the nature of the dihydride species? What role do defects play?

We have performed time-of-flight measurements on D_2 desorbed from Si(100) and Si(111) surfaces which have been reported briefly elsewhere.[33] In addition, molecular beam experiments have been carried out in an attempt to measure directly the sticking probability of molecular hydrogen (D_2) and its dependencies on surface and molecular temperatures. Combining these results with the internal state distributions of Kolasinski, Shane, and Zare,[22] we are able to calculate the energy content of hydrogen thermally desorbed from Si. Hence, by invoking energy conservation and the principle of detailed balance,[34–37] we are able to estimate the height of the barrier to adsorption.

From the data presented here, we conclude that the desorbed molecules do not possess a great excess of energy compared to the equilibrium expectation at the temperature of the thermal bath. Thus, along the desorption trajectory, the desorbing molecules do not pass over a barrier in the molecule–surface coordinate with an energy significantly in excess of the zero point of energy associated with the free molecule–surface system. In other words, the desorbed molecules do not show any sign of having traversed a barrier that can be associated with a barrier to adsorption which could in turn explain the lack of molecular hydrogen adsorption.

It is well-known in the literature that the sticking coefficient of a room-temperature sample of molecular hydrogen is vanishingly small. An upper limit for this value of $\approx 10^{-8}$ can be drawn from the work of Liehr *et al.*[38] No measured value for the sticking coefficient is available; nor are there any extant determinations of the dependence of this parameter on molecular energy or T_s. Nonetheless, it has long been assumed that a substantial barrier to adsorption is responsible for the low sticking coefficient. The results presented here directly demonstrate that translational and/or internal energy of the incoming molecules aids in overcoming a barrier toward adsorption. However, more importantly, these data demonstrate that dissociative adsorption is activated by thermal excitation of the lattice. From the observed T_s dependence of S, we confirm our earlier speculation[33] that the surface atom configuration plays a decisive role in the adsorption/desorption dynamics.

II. EXPERIMENT

Experiments were performed in an ultrahigh vacuum (UHV) chamber with a base pressure of $<2\times10^{-10}$ mbar which is pumped by ion, turbo, and Ti-sublimation pumps as well as by l-N_2-cooled panels. Details of this apparatus, which are depicted schematically in Fig. 1, are described elsewhere.[39] Si(100) (As-doped, 0.005 Ω cm, <0.5° miscut) and Si(111) (n-doped, 8–10 Ω cm, <0.5° miscut) crystals were prepared as described previously[22] and yielded sharp low energy electron diffraction (LEED) patterns of the appropriate symmetry. The temperature of the crystals was monitored by chromel–alumel thermocouples and calibrated with an optical pyrometer. One Si(111) and four different Si(100) crystals were used during the course of these studies.

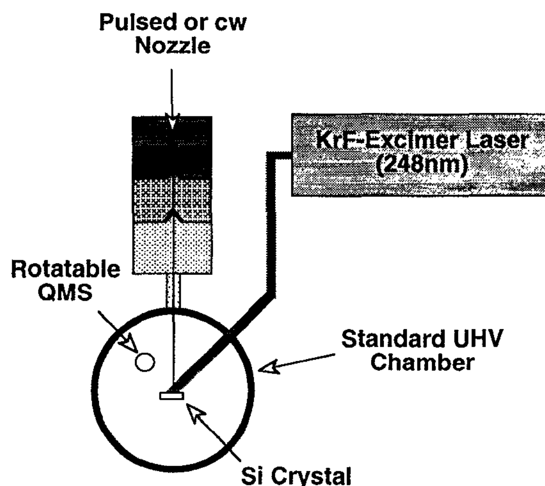

FIG. 1. A schematic drawing of the experimental apparatus.

Atomic hydrogen (D) dosing for the time-of-flight (TOF) studies and for coverage calibration was accomplished by backfilling the chamber with D_2 to 2×10^{-6} mbar, while heating a W filament to approximately 1900 K. The W filament was thoroughly outgassed and the inner walls of the chamber were l-N_2 cooled prior to dosing to avoid contamination of the crystal during exposure. The crystal temperature during exposure was held at ≈400 K to suppress H-atom-induced etching. In experiments involving the monohydride alone, the crystal was first annealed to desorb the dihydride. The saturation coverage of the monohydride phase was assumed to be one monolayer (1 ML$=6.78\times10^{14}$ cm^2). The crystal temperature was held at 600 K idle temperature during the laser induced thermal desorption (LITD) experiments. All LITD experiments were initiated at saturation coverage for the appropriate phase.

Time-of-flight measurements were performed by means of LITD. These results have been reported previously[33] and will only be briefly summarized here. A KrF excimer laser operating at 248 nm [5 Hz repetition rate, 17 ns full width at half-maximum (FWHM) pulses] produced the temperature jump required for desorption. Fluences between 140 and 350 mJ cm^{-2} were utilized, which lead to peak surface temperatures in the range 920–1520 K. No mass 4 signal was observed for laser powers which did not heat the crystal sufficiently above the thermal desorption temperature of deuterium. Sample to ionizer distances of 25–75 mm were employed and TOF spectra were corrected for ion flight times within the quadrupole mass spectrometer (Balzers QMG 311, 5° angular resolution) used for detection.

Pulsed and continuous molecular beams were utilized to investigate the adsorption of molecular D_2. The pulsed nozzle (General Valve, Series 9) has a diameter of 275 μm and was operated at 1–25 Hz delivering ~1 ms pulses. The

continuous nozzle consists of a stainless steel body and a 65 μm diameter Pt electron microscope objective which defines the orifice. The cw nozzle could be heated to temperatures T_n in the range 300–1040 K. Stagnation pressures of 2–4 bar (pulsed nozzle) and 1–2 bar (cw) were employed. Before entering the main chamber, the molecular beam passes through two diffusion-pumped stages which contain adjustable apertures for beam collimation and cross-sectional area control. In all results presented here, the apertures were chosen such that the entire crystal was illuminated by the molecular beam. Experiments in which the beam contacted only a small section of the Si surface exhibited similar behavior.

Two types of beam experiments were performed. In the first, D_2 was introduced using the cw beam, with the angle of incidence along the sample normal. In these experiments, T_s and T_n were varied for a given exposure of D_2. Exposure times were varied from 1 to 90 min. The dependencies on T_s and T_n were measured with exposures of 10–15 min. During exposure, all filaments and the ion pump were turned off to avoid possible atomization of D_2 and misleading adsorption resulting from atomic deuterium. After exposure, temperature programmed desorption (TPD) either for mass 4 (D_2) or 44 (SiO) was performed. Control experiments to determine the effects of background adsorption were conducted in which the surface was turned away from the molecular beam, while the molecular beam was allowed to enter the main chamber. At exposure times up to 60 min, no observable oxygen or deuterium adsorption was recorded.

We did, however, measure a persistent mass 44 signal after exposure of the surface to the beam, which is the result of SiO desorption (the possibility that some of the mass 44 signal, especially at temperatures >1000 K, comes from CO_2 desorption from the crystal holder cannot be ruled out). This indicates that a small amount of oxygen, typically on the order of 0.02 ML, is present on the surface as the result of either O_2 or D_2O adsorption. We expect the O_2:D_2O ratio to be T_n dependent (see below); however, the mass 44 desorption signal was found to correlate with *neither* T_s *nor* T_n. The estimated background level presented in the figures is calculated based on the assumption that all of the mass 44 signal is the result of D_2O adsorption (worst-case scenario).

We can rule out an intrinsic D_2O impurity in our beam because we used a l-N_2 cold trap to freeze out impurities. However, O_2 will not be eliminated by such a trap, and since we are using such large throughputs of gas (on the order of 10^3–10^5 L), traces of O_2 (resulting from leaks, impurities in the gas supply, and desorption from the gas-handling-system walls) on the order of a few parts per million will be detected in our TPD results. Extreme measures were taken to eliminate all possible leaks; however, we could not get rid of the exceedingly small amount of oxygen left in the beam.

Formation of D_2O or atomic D in the nozzle will lead to a spurious D_2 desorption signal. We have calculated[40] the atomic D fraction to be $\leqslant 10^{-8}$ at $T_n = 1000$ K and it is, therefore, negligible. With the nozzle at room temperature, the D_2O formation reaction should be slow and it is likely that not all of the O_2 is converted to D_2O. However, at the elevated nozzle temperatures used in this study (700–1040 K), the Pt nozzle tip will with high efficiency catalyze the formation of D_2O. At elevated T_n, the possibility of reaction between D_2 and oxides present on the inner walls of the nozzle also exists. The catalytic formation of D_2O is likely one cause of the larger error bars in the S vs T_n data reported here as compared to the measurements conducted with a room temperature nozzle.

A second source of error was related to the difficulty of regulating the flux through the heated nozzle due to clogging. With little difficulty, we were able to acquire data within one day which was self-consistent and led to reproducible trends. However, day-to-day comparisons varied with respect to one another in their absolute values as can be seen in the rather large error bars (one standard deviation for up to nine independent measurements) reported in Fig. 3. Furthermore, the relative precision of the data is reflected in the error bars; however, the accuracy of the absolute values is suspected to be good to within a factor of 2–3. The cause of this range in the absolute accuracy stems from the estimates of beam flux. These estimates are dependent on the value of the pumping speed for which we have only an estimated and not a measured value. The beam flux was estimated by measuring the molecular-beam-induced pressure rise in the main chamber while it was pumped by the turbo pump alone. From the equilibrium pressure, typically 5×10^{-8} mbar, and the (assumed known) pumping speed, 100 $\ell\,s^{-1}$, we calculate the incoming flux 3.5×10^{15} molecules $cm^{-2}\,s^{-1}$.

The second set of beam experiments was carried out for sample temperatures well beyond the temperature at which hydrogen desorption occurs at a rate faster than 1 ML s^{-1}. Such experiments were expected to test the transient dissociative adsorption of molecules. A H_2/D_2 mixture was introduced into the pulsed nozzle. The beam was incident upon the surface at 45° to the sample normal. The crystal could be held at an arbitrary temperature in the range $100 \leqslant T_s \leqslant 1200$ K. The experimental concept is that if the H_2 and D_2 molecules adsorb dissociatively and diffuse on the surface prior to recombinative desorption, isotopic mixing should occur and HD will be formed. The surface temperature could also be pulsed so as to create temperature jumps from an idle temperature of, e.g., 1000 K to a preset temperature in the range 1000–1500 K. For this purpose, a set of large capacitors were charged to a maximum of 75 V and, with a repetition rate of 1 Hz, discharged through the sample heating circuit using a high power switching unit. The resulting heater current pulse through the sample (~170 A, ~20 ms) raised T_s by up to 500 K in 20 ms followed by cooling to the idle temperature on a time scale of 500 ms. Such a procedure avoids excessive heating of the sample holder assembly, which would result in outgassing. The temperature was monitored using a fast pyrometer (Kleiber type 270A-I, Si chip detector, 300 μs rise time). The sample quality was checked by LEED after running the experiment in this mode for long periods and showed an excellent pattern. The pulsed nozzle was triggered such that the gas pulse hit the surface at the peak temperature. The QMS was tuned to mass 3 and positioned along the sample normal. The HD signal before the pulse is compared with the HD signal at the peak of the temperature jump. In this way, we are able to discriminate

TABLE I. Observed values of the mean translational energy $\langle E_{trans}\rangle/2k$ for D_2 desorbed from Si surfaces.

	Desorption conditions		$\langle E_{trans}\rangle/2k$ (K)
(i)	Si(100)-(2×1):D	T_{max}=920 K	960±200
(ii)	Si(100):2D	T_{max}=920 K	990±180
(iii)	Si(111)-(7×7):D	T_{max}=1520 K	1300±440

against the HD impurity present in the beam before interaction with the surface.

III. RESULTS

A. Laser induced thermal desorption

The results of LITD experiments have been reported previously[33] and are summarized here. Table I contains values of the mean translational energy $\langle E_{trans}\rangle/2k$ for D_2 desorbed from Si surfaces extracted from over 600 TOF distributions. Data were collected for three sets of experimental conditions: (i) monohydride-covered Si(100)-(2×1) laser heated to a maximum temperature T_{max} of 920 K; (ii) mixed mono- and dihydride-covered Si(100) laser heated to T_{max}=920 K; and (iii) monohydride-covered Si(111)-(7×7) laser heated to T_{max}=1520 K. In Table II are listed calculated[41] values of T_{max} and the flux-weighted mean desorption temperature $\langle T_{des}\rangle$. Since desorption occurs throughout the laser pulse, a range of surface temperatures contribute to the desorption flux. The range of significant surface temperatures can be estimated from the values in the last two columns of Table II. In these columns are listed values of the range of surface temperatures about $\langle T_{des}\rangle$ in which 85% and 98% of desorption occurs. From these values, we can see that some smearing of the desorption temperature on the order of ±(15–50) K about $\langle T_{des}\rangle$ is expected.

By comparing the values in Tables I and II, we conclude that for all three experimental cases, the value of $\langle E_{trans}\rangle/2k$ does not deviate, within error bars, from T_s during desorption. The results can be interpreted in terms of the translational energy being fully to nearly fully accommodated with T_s. However, because of the substantial error bars on these values, one could also state that the translational energy was, in effect, constant for the three cases at a value of roughly 1000 K. We favor the former interpretation; however, assumption of the latter interpretation will change none of the argumentation in this work. In either case, we can conclude that the mean translational energy of the desorbed molecules is independent of both surface and adsorbate structure. In addition, we note that during the LITD experiments the coverage is depleted with each laser pulse at a rate dependent on the laser fluence. Within error bars, we observed no change in the TOF spectra as a function of the number of incident laser pulses; therefore, we do not observe any systematic changes in the translational energy as a function of coverage. Any dependence of $\langle E_{trans}\rangle$ on coverage is, if at all present, hidden within our error bars.

TABLE II. Calculated values of the maximum surface temperature achieved during LITD T_{max}, the desorption-flux-weighted mean desorption temperature $\langle T_{des}\rangle$, and the temperature ranges around T_{des} in which 85% of the desorption occurs and in which 98% occurs.

T_{max} (K)	$\langle T_{des}\rangle$ (K)	85%	98%
920	900	+20/−5	+20/−65
1520	1480	+40/−50	+40/−175

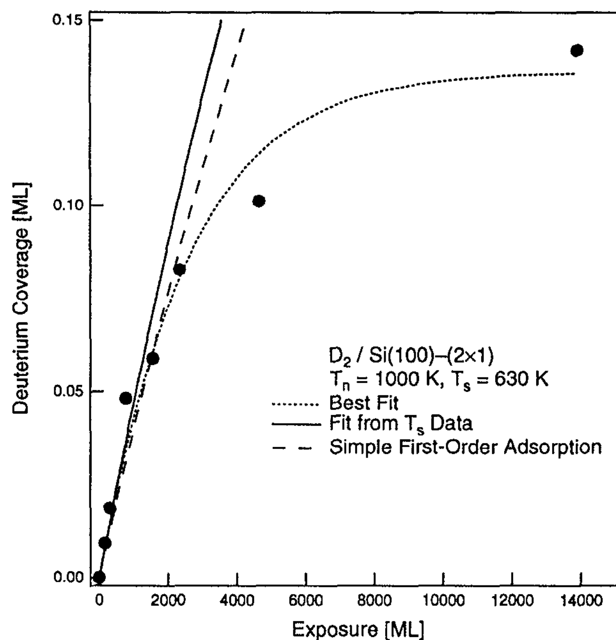

FIG. 2. Deuterium coverage vs D_2 exposure expressed in monolayer equivalents. The dashed line represents a fit to the first six data points assuming simple Langmuirian adsorption kinetics alone. The dotted line represents the best fit to the exposure data allowing for concurrent adsorption and desorption by applying modified first-order kinetics (Ref. 19). The solid line represents a fit to modified first-order kinetics derived from the data in Fig. 4.

B. Adsorption measurements as a function of coverage

To explore the sticking coefficient as function of nozzle and sample temperature, we start with an uptake curve for D_2 adsorption on Si(100)-(2×1) (Fig. 2). These data were obtained by exposing a surface held at T_s=630 K to a molecular beam of D_2 at a nozzle temperature of T_n=1000 K for various lengths of time (1–90 min). The calculated mean translational energy of the D_2 beam is $\langle E_{trans}\rangle(D_2)$=233 meV. The vibrational temperature of this beam should be ~1000 K ($N_{v=1}/N_{v=0}$=0.013), whereas the rotational temperature should be somewhat below 1000 K. The conditions yield the largest sticking observed.

The data show an uptake of molecular hydrogen which saturates for large exposures at a coverage of 0.14 ML. We delay further discussion until all data have been presented.

In principle, all measurements of sticking dependencies on T_n and T_s should also be carried out in the same manner as for the data displayed in Fig. 2. This would allow us to compare directly the extrapolated values of $S_0(T_n,T_s)$. This, however, was not practicable because S drops significantly

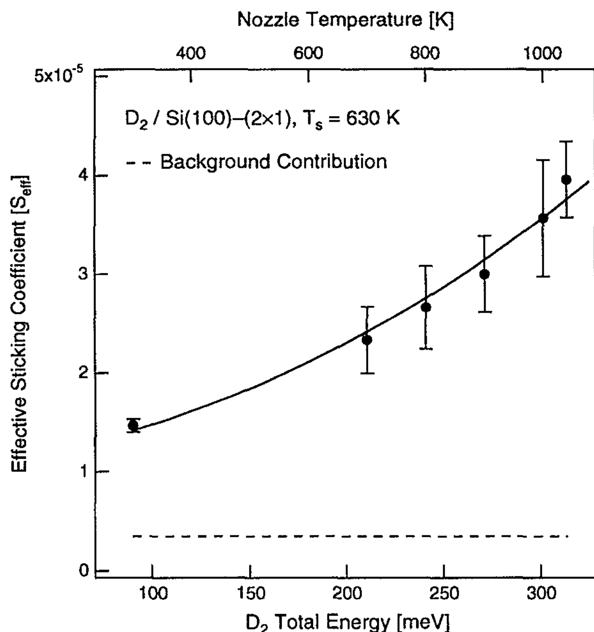

FIG. 3. The effective D_2 sticking coefficient as a function of incident energy. The solid line represents the results of a simultaneous best fit to these data and those in Fig. 4. The dashed line represents the estimated contribution of background adsorption.

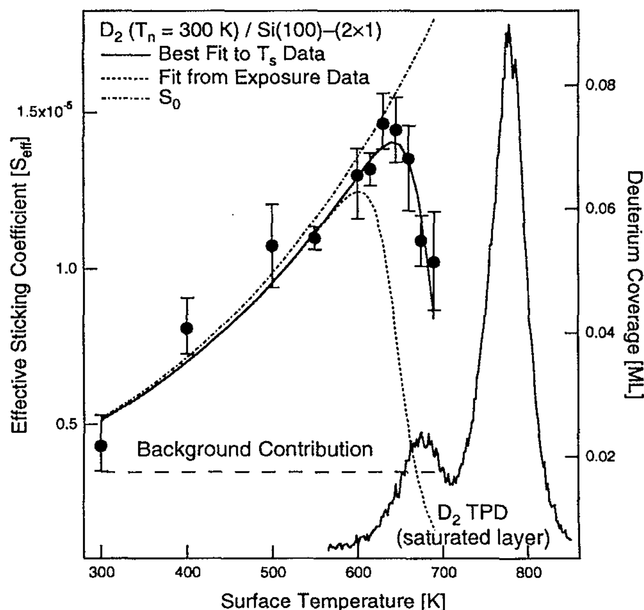

FIG. 4. The dependence of the effective sticking coefficient on surface temperature. The solid line represents the best fit to modified first-order kinetics (Ref. 19). The dotted line represents a fit using the desorption activation energy derived from the data in Fig. 2. The dotted–dashed line represents the value of S_0 derived from the best fit. The estimated background contribution is denoted by the dashed line.

for lower values of T_s and T_n. Therefore, we elected to perform experiments for a fixed exposure, which under our beam flux conditions amounted to 10–15 min. These exposures led to the adsorption of $\leqslant 0.09$ ML of D atoms (depending on T_s and T_n). While the difference is not great, it should be kept in mind that the effective sticking coefficients S_{eff} reported in the following two sections are integrated sticking coefficients for a small finite coverage rather than S_0.

C. Adsorption measurements as a function of nozzle temperature

The results of measurements performed to determine the dependence of the effective sticking coefficient—$S_{eff} = \theta/(Ft)$, where F is the flux of molecules onto the surface—on nozzle temperature are displayed in Fig. 3. The total beam energy could be varied between 90 and 315 meV. The surface temperature was held at 630 K for this series of experiments. We clearly observe an increase of the sticking coefficient by a factor of 3 with increasing T_n. *This increase in S unambiguously indicates that the adsorption process is activated*; however, from these data alone, we cannot determine whether increased translational or vibrational energy is more important or what the individual efficacies of translational and vibrational energies are. Such detailed experiments were not feasible with the present apparatus. Within the range of accessible beam energies we do not observe saturation of the sticking.

D. Adsorption measurements as a function of surface temperature

The data for S_{eff} measured as a function of T_s for a 300 K D_2 beam ($\langle E_{tot}(D_2)\rangle = 90$ meV; $\langle E_{trans}(D_2)\rangle = 65$ meV; $T_{vib} \approx 300$ K; $T_{rot} \leqslant 300$ K) are displayed in Fig. 4. The effective sticking coefficient is observed to rise from a value insignificantly larger than the background level to a maximum of $(1.5 \pm 0.1) \times 10^{-5}$ at $T_s = 630$ K. *The increase in the sticking coefficient with increasing T_s clearly indicates that hydrogen adsorption is activated in the coordinates of the surface.* For higher sample temperatures, the amount of adsorbed hydrogen which is observed in TPD after exposure to the beam decreases. This decrease of the residual coverage is correlated with the onset of thermal desorption as observed in TPD. A typical TPD spectrum is also shown in Fig. 4. One has to keep in mind that even desorption rates on the order of 10^{-3} ML s^{-1} have an effect on these curves considering the typical exposure times of 15 min. As will be shown below, it cannot be concluded whether desorption out of the dihydride state is responsible for the decrease of effective sticking, as may appear likely on first glance.

We have also attempted to measure the sticking coefficient for dissociative adsorption at T_s much greater than the TPD peak temperature. These experiments were performed by using a mixed H_2/D_2, 300 K supersonic molecular beam incident on a Si surface pulse heated to $T_s = 1000-1500$ K. We then attempted to detect any HD produced as the result of dissociative adsorption followed by recombinative desorption. The HD signal (on the order of 1200 counts) was measured before and during the heating pulse. The former was

subtracted from the latter to yield the net amount of HD produced by the interaction of the H_2/D_2 beam with the surface. We typically measured a difference signal 0 ± 30 counts of HD and 3×10^5 counts of D_2. Accordingly, the upper limit on the fraction of the incident beam converted to HD by isotopic scrambling is $<1\times10^{-4}$ for $300\leq T_s\leq1500$ K.

IV. DISCUSSION

A. Adsorption results

The adsorption experiments presented here demonstrate unambiguously that hydrogen adsorption on Si(100) is activated. Although this has been assumed for some time, the data presented here represent the first direct experimental evidence for this behavior. Furthermore, both increased molecular energy and increased sample temperature enhance adsorption. These results demonstrate that not only the translational and vibrational degrees of freedom of the molecule, but also lattice excitations play important roles in the adsorption process.

This combined dependence has some important consequences for the data analysis. For part of the data, it has to be taken into account that adsorption is in competition with thermal desorption during the course of the experiment, as is obvious from the data presented in Fig. 4. Hence, the resulting coverage by the end of the exposure time must be calculated by integrating the following rate equation:

$$\frac{d\theta(t)}{dt}=R_{\mathrm{ads}}-R_{\mathrm{des}}, \tag{1}$$

where R_{ads} and R_{des} are the rate of adsorption and desorption, respectively. The rate of adsorption is described by

$$R_{\mathrm{ads}}=S_0(T_s,T_n)f[\theta(t)]F, \tag{2}$$

where $S_0(T_s,T_n)$ is a surface and nozzle temperature dependent initial sticking coefficient, $f(\theta(t))$ represents the coverage dependence of the sticking coefficient, and F is the flux of molecules onto the surface.

The rate of desorption is assumed to follow a Polanyi–Wigner equation

$$R_{\mathrm{des}}=\theta(t)^n k_d=\theta(t)^n A_d \exp\left(-\frac{E_d}{kT}\right), \tag{3}$$

where n is the reaction order, k_d is the desorption rate constant, A_d is the Arrhenius prefactor, E_d is the desorption activation energy, and k is the Boltzmann constant.

Only for low sample temperatures ($T_s\leq630$ K) and exposure times ≤15 min is the term resulting from desorption negligible. Fortunately, it turns out that the adsorption parameters can be determined with sufficient accuracy from the data at and below this temperature alone.

1. Adsorption measurements as a function of coverage

These data, displayed in Fig. 2, were fitted to simple Langmuir adsorption kinetics of the form

$$\theta(t)=\theta_{\max}\left[1-\exp\left(-\frac{S_0Ft}{\theta_{\max}}\right)\right], \tag{4}$$

where $\theta(t)$ is the deuterium coverage at time t, $\theta_{\max}$ is the saturation coverage, S_0 is the sticking coefficient at zero coverage, F is the D_2 flux incident on the surface expressed in ML equivalents s^{-1}, and the coverage dependence of the sticking coefficient is assumed to follow $f(\theta)=[(1-\theta)/\theta_{\max}]$. The dashed line in Fig. 2 represents a fit over the first six data points to Eq. (4) assuming that $\theta_{\max}=1$ ML, as would be expected for the monohydride phase. For these data points, the influence of competing desorption can be neglected, since the coverage is small. Note, however, that $\theta_{\max}=1$ ML represents the saturation coverage for the monohydride phase produced as the result of exposure to atomic hydrogen and, therefore, it need not represent the saturation coverage due to molecular hydrogen exposure. This fit indicates that the adsorption process (at low coverage) can be described by a simple Langmuir isotherm and that $S_0(T_s=630\text{ K}, T_n=1000\text{ K})=(5\pm1)\times10^{-5}$. It is noteworthy that the first six points of the curve can be equally well described by assuming $f(\theta)=[(1-\theta)/\theta_{\max}]^2$, which results in the same value of S_0. For simplicity, we will refer to the former case as first-order adsorption kinetics and the latter as second-order adsorption kinetics.

It remains, however, to explain the behavior of the entire curve. First we note that this may be an effort in futility because the oxygen coverage present on the surface for the final data point, which was recorded for an exposure time of 90 min, is estimated to be ≈0.06 ML. The presence of oxygen could affect the adsorption/desorption kinetics. With this caveat, the entire curve can be fitted by assuming $\theta_{\max}=0.14$ ML. While the fit is excellent, this mathematical solution begs the physical explanation of such a low saturation coverage. We believe that concurrent desorption or desorption in combination with a value of $\theta_{\max}<1$ ML for the adsorption of molecular hydrogen to be the cause of this behavior. Such a conclusion is indeed suggested by the data presented in Fig. 4 and we, therefore, discuss this point in greater detail below in combination with the data from Fig. 4.

In all subsequent fits, $\theta_{\max}$ was held constant at 1 ML. Because the data treated below were obtained in the low coverage regime, $\theta_{\max}$ does not influence the fits as long as its value is above 0.25 ML.

2. Adsorption measurements as a function of nozzle temperature

We have observed that sticking increases with increasing nozzle temperature. Because the data have been obtained for $T_s=630$ K, desorption can be neglected. This assumption has also been checked and shown to be valid analytically. For clarity of presentation, we consider only adsorption.

Because the data are only taken over a small range of energies ($300\leq T_n\leq1040$ K $\Rightarrow 90.5\leq E_{\mathrm{tot}}\leq314$ meV), because S increases only by roughly a factor of 3 without any indication of saturation, and because the error bars are so large, fitting of the data is precarious and the results must be interpreted with caution. The results can be successfully fitted using error functions as suggested by Rettner, Michelsen, and Auerbach[42,43]

$$S_{\mathrm{eff}}(E_{\mathrm{tot}})=s_1+\frac{A'}{2}\left[1+\mathrm{erf}\left(\frac{E_{\mathrm{tot}}-E_{\mathrm{barrier}}}{W_{\mathrm{barrier}}}\right)\right], \tag{5}$$

where s_1 is a constant which can, for instance, account for background adsorption (and has, therefore, been set equal to 4×10^{-6}), A' is the saturation value of the sticking coefficient at high beam energy (thus equal to 0–1), E_{tot} is the total energy of the incident molecule, E_{barrier} is the adsorption barrier, and W_{barrier} is the width parameter for E_{barrier}.

Using a single function of the form of Eq. (5), i.e., assuming that the sticking coefficient is a function of total energy of the incident molecules leads to a satisfactory fit. Equally good, nonetheless underdetermined, fits are obtained by assuming, in analogy to the hydrogen/Cu case,[42,43] that $S(E)$ is a function of translational energy alone, with different barrier heights for the vibrational states $v=0$, 1, and 2. Because of the limited data set, we cannot differentiate between these two cases and we report only the former values.

The fit displayed in Fig. 3 corresponds to the parameter set $A'=1\times10^{-3}$, $E_{\mathrm{barrier}}=1.06$ eV, and $W_{\mathrm{barrier}}=0.60$ eV. A strict constraint on the values of A', E_{barrier}, and W_{barrier} can only be obtained by the observation of saturation in the S_{eff} vs T_n data. Unfortunately, we were unable to probe sufficiently high beam energies to observe saturation. We have varied the fit parameters through a wide range of values and report here what we believe to be the best family of values—a set of parameters that allows a simultaneous fit of all of the presented data.

Nonetheless, these results unambiguously indicate that hydrogen adsorption is activated in the molecule–surface coordinate. This finding is consistent with the results of KSZ, who found that hydrogen desorption results in a hyperthermal population of the $v=1$ state. Moreover, the fit indicates a broad distribution of barrier heights ($\approx$0.6 eV) about a large mean value ($\approx$1 eV). This wide range of barrier heights may also be taken as a first indication of the importance of surface atom configurations in the adsorption process. That is, the impact point within the unit cell and thermal motion of the surface atoms will result in a range of adsorption barriers being presented to an incident hydrogen molecule, and this will be reflected in a large value for W_{barrier}. Moreover, the fit seems to indicate that at this sample temperature (630 K), the sticking coefficient is limited to $\leqslant10^{-3}$ whatever the beam conditions are chosen to be.

3. Adsorption measurements as a function of surface temperature

We now attempt to fit concurrently the θ vs exposure and S_{eff} vs T_s data as well as the S_{eff} vs T_n data by calculating the simultaneous effects of adsorption and desorption. Assuming that the T_s and T_n barriers are essentially independent of one another (which we can justify when we consider how inefficient impulsive energy transfer from hydrogen to the lattice should be), we can express the sticking coefficient as

$$S_0(T_s,T_n)=s_1+\frac{s_2(T_s)}{2}\left[1+\mathrm{erf}\left(\frac{E_{\mathrm{tot}}-E_{\mathrm{barrier}}}{W_{\mathrm{barrier}}}\right)\right] \tag{6}$$

and

$$s_2(T_s)=\frac{A}{2}\left[1+\mathrm{erf}\left(\frac{kT_s-E_a}{W_a}\right)\right], \tag{7}$$

where we have extended Eq. (5) to include an additional term, describing activation by T_s, formally as a T_s-dependent adsorption barrier, defined by its height E_a along with a corresponding width parameter W_a. This equation could also be interpreted to describe a T_s dependent maximum sticking coefficient, i.e., $A'=s_2(T_s)$. The net effect is the same as when E_{barrier} would decrease with increasing T_s.

We have attempted to fit the data in Figs. 2 and 4 to all combinations of first- and second-order behavior, as well as the modified first-order kinetics suggested by D'Evelyn, Yang, and Sutcu.[19] Regardless of the assumptions made concerning the desorption kinetics, we consistently obtain a single set of adsorption parameters which describe the data. The fit in Fig. 4 corresponds to $s_1=5\times10^{-7}$, $A=1$, $E_a=0.32$ eV, and $W_a=0.12$ eV, and the same values of E_{barrier} and W_{barrier} used in Fig. 3.

In the fitting procedure, it is important to note two points. First, the value of A' in Eq. (5) is not free. It is constrained by the T_s data [cf. Eqs. (6) and (7)]. Therefore, A' is determined not only by the data in Fig. 3, but also the data in Fig. 4, and it is, therefore, essential to determine the T_s dependence of the sticking coefficient to be able to interpret completely the T_n data. Second, the dependence of A' on both sets of data leads to an analytical coupling between $\{E_{\mathrm{barrier}},W_{\mathrm{barrier}}\}$ and $\{E_a,W_a\}$. We have found that a range of combined values can lead to good fits. From this range of suitable fit parameters, we arrive at

$$s_1=(2\pm2)\times10^{-6}\quad A=0.9-1,$$

$$E_a=0.31\pm0.04\ \text{eV},\quad W_a=0.11\pm0.02\ \text{eV},$$

$$A'(T_s=630\ \text{K})=(1.0\pm0.3)\times10^{-3},$$

$$E_{\mathrm{barrier}}=(1.0\pm0.2)\ \text{eV},$$

$$W_{\mathrm{barrier}}=(0.6\pm0.1)\ \text{eV}.$$

The value of s_1 is found to be of little importance for fitting the T_s data. Setting it to any value between 0 and 4×10^{-6} leads to values of the other parameters within the above reported ranges.

A difficulty arises, however, in attempting to settle on a consistent set of desorption parameters which can describe the data in Figs. 2 and 4. We note that desorption plays a negligible role for the first six data points in both sets of data and, therefore, we have a sufficient set of data points for the determination of the adsorption parameters from these data alone.

Both complete sets of data in Figs. 2 and 4 can be fitted with virtually the same set of parameters if desorption is assumed to be second order. In this case, we arrive at (expressed in first-order units) $A_d=(2.5\pm1)\times10^{13}$ s^{-1} and $E_d=2.0\pm0.03$ eV. Second-order kinetics and $E_d=2.02\pm0.02$ eV have been reported for desorption at high coverage for the dihydride species on Si(100).[44] However, in this case, $A_d\approx2\times10^{15}$ s^{-1}, which differs considerably from the value obtained here. Note also that the kinetics of dihydride de-

sorption are still controversial and that first-order kinetics with coverage-dependent values of A_d and E_d have yet to be ruled out.

Simple first-order kinetics yield a best fit to the data in Fig. 4 with a similar value of E_d (1.98 eV), but with an even lower Arrhenius prefactor (5×10^{11} s^{-1}). The fit to the exposure data of Fig. 2, on the other hand, leads to $A_d=2\times10^{12}$ s^{-1} and $E_d=1.92$ eV. We conclude that simple first-order adsorption and desorption do not adequately describe the data.

Applying modified first-order kinetics with the dimer stabilization energy suggested by Höfer, Li, and Heinz[5] to reflect the influence of pairing, we arrive at the fit corresponding to the solid line displayed in Fig. 4 with $A_d=(2\pm1)\times10^{15}$ s^{-1} and $E_d=2.44\pm0.03$ eV. These values agree within error bars with those obtained for desorption from the monohydride species.[3,5,44] These desorption parameters, in combination with the adsorption parameters listed above, also adequately fit the first six data points in Fig. 2. From the best fit to the data in Fig. 2, however, we arrive at $A_d=(2\pm1)\times10^{15}$ s^{-1} and $E_d=2.31\pm0.03$ eV.

We conclude that adsorption is activated in the surface coordinates and that the increase of the sticking coefficient as a function of T_s indicates that the saturation value of the sticking coefficient is near unity and the apparent barrier height is 310 ± 40 meV with a broad width of $W_a=110\pm20$ meV. The conclusions concerning the desorption process are somewhat ambiguous. We may be observing desorption from a dihydride intermediate state. On the other hand, the data are also consistent with the proposition that the desorption process which is influencing our measurements is desorption from the monohydride state and that the influence of coadsorbed oxygen is responsible for lower E_d obtained from the fit to the data in Fig. 2.

For a mixed H_2/D_2 beam, the probability for isotopic mixing in the range $300\leq T_s\leq1500$ K is $<1\times10^{-4}$. To interpret this result, we must consider the residence time of adsorbed deuterium and the rate of diffusion to determine the probability of isotopic scrambling. These factors must be considered because as the steady-state coverage approaches zero, the probability of isotopic scrambling also approaches zero because it is more probable that a hydrogen atom will recombine with its original partner before it can find a "foreign" hydrogen atom. Taking this into consideration, we find that $S_0<10^{-1}-10^{-2}$ for $300\leq T_s\leq1500$ K. This result is consistent with an extrapolation to high T_s of the data in Fig. 4.

B. Desorption results

The measurement of the total energy of desorbed molecules represents a method of estimating the magnitude of the adsorption barrier. As we have argued previously,[33] the energy content of an ensemble of desorbed molecules is derived from two contributions. The first contribution arises from equilibration in the heat bath provided by the surface. This quantity we denote E_{eq}. The second contribution arises if there is an activation barrier to adsorption. This barrier must also be crossed in desorption if the same path along the potential energy hypersurface is followed in the two reactions. A light molecule such as hydrogen exchanges virtually no energy with the surface as it comes down off this barrier. Therefore, the energy from overcoming this barrier E_0 remains in the desorbed molecules until they are detected in the gas phase. Hence for a system which exhibits activated adsorption, the flux of desorbed molecules have a mean energy content $\langle E_{flux}\rangle$ given by

$$\langle E_{flux}\rangle\approx E_{eq}+E_0. \tag{8}$$

If we neglect the small energy loss which is expected to occur in the exit channel during desorption, we can assume Eq. (1) to be an equality. Substituting the mean energy of the desorbed flux $\langle E_{flux}\rangle=\langle E_{trans}\rangle+\langle E_{rot}\rangle+\langle E_{vib}\rangle$ $(=2kT_{trans}+kT_{rot}+kT_{vib}$ for a Boltzmann distribution), and the equilibrium contribution to the energy $E_{eq}=4kT_s$, we obtain for the height of the activation barrier to adsorption

$$E_0=\langle E_{trans}\rangle+\langle E_{rot}\rangle+\langle E_{vib}\rangle-4kT_s. \tag{9}$$

The experimentally determined values of the internal and translational temperatures are given in Table III.

TABLE III. Observed values of the mean rotational $\langle E_{rot}\rangle$ and translational $\langle E_{trans}\rangle$ energies and the vibrational temperature T_{vib} for D_2 desorbed from Si and Cu surfaces.

T_s (K)	$\langle E_{rot}\rangle$ (K)	T_{vib} (K)	$\langle E_{trans}\rangle/2k$ (K)	E_0(meV) [from Eq. (9)]
Si(100): 780	330±50[a]	1700±350[a]		77±80
Si(100): 900			960±200[b]	
Si(111): 1480			1300±440[b]	
Cu(111): 925[c,d]	1020	1820	3360	505

[a]K. W. Kolasinski, S. F. Shane, and R. N. Zare, J. Chem. Phys. **96**, 3995 (1992).
[b]This work.
[c]H. A. Michelsen, C. T. Rettner, D. J. Auerbach, and R. N. Zare, J. Chem. Phys. **98**, 8294 (1993).
[d]H. A. Michelsen, C. T. Rettner, and D. J. Auerbach, Phys. Rev. Lett. **69**, 2678 (1992).

In order to calculate E_0 from Eq. (9), we must extrapolate the value of $\langle E_{trans}\rangle$ measured here to a surface temperature of 780 K to compare with the data of KSZ measured at this T_s. Within error bars, we observe $\langle E_{trans}\rangle/2k=T_s$ at the two values of T_s probed experimentally. However, the exact nature of the scaling has not been determined and we therefore assume $\langle E_{trans}\rangle/2k=960$ K at $T_s=780$ K. This marginally increases the estimate of E_0 provided by Eq. (9) compared to assuming full accommodation of the translational energy. Substituting the appropriate values into Eq. (9), we obtain

$$E_0\leq77\pm80 \text{ meV}.$$

Note that we would have to measure $\langle E_{trans}\rangle/2k\approx6500$ K to obtain a barrier height of 1 eV. We conclude that *the desorbed molecules show no evidence for a large barrier to adsorption.* As a means of comparison and a check for this method of estimating E_0, the same calculation has been performed for Cu(111). These results are collected in Table III. By comparing the value obtained from Eq. (9) (505 meV) to the most recent estimate of Rettner, Michelsen, and

Auerbach[43] (~0.5 eV), we may conclude that Eq. (9) provides a good estimate of the effective E_0 traversed along the desorption trajectory.

At this point, we must reflect on these results. An implicit assumption in Eq. (8) is that virtually all of the excitation in the transition state is transferred to the desorbing molecules rather than to the surface. For the H/Cu system, this assumption is shown to be valid as a result of the good agreement between the value obtained from Eq. (8) and the experimentally determined value. In this case, the results of desorption and adsorption experiments clearly agree with one another and demonstrate that it is the excitations of the hydrogen molecule which are important in overcoming the barrier to adsorption. Furthermore, it is the latter excitations which carry away virtually all of the energy of the activated complex in desorption.

For H/Si, however, the agreement between adsorption and desorption results is miserable. We have demonstrated in Sec. III C that hydrogen excitations *can* aid in overcoming an adsorption barrier of ≈ 1 eV. However, such a result is only obtained at elevated sample temperature and sticking is still limited to $\leqslant 10^{-3}$. Nonetheless, desorbed molecules *do not* show indications of having traversed such a large barrier. Therefore, there must exist trajectories for which that portion of the adsorption barrier which affects molecular excitations (E_0) is small. This does not mean that there is no adsorption barrier at all for these trajectories. Indeed, in Sec. III D, we have demonstrated that adsorption is activated by surface excitations (T_s). The actual adsorption barrier probed by the molecule must be dependent on surface excitations. This apparent barrier in surface degrees of freedom (≈ 310 meV), however, does not transfer energy to the desorbing molecules and, therefore, it is localized in the coordinates of the surface.

Pulling all of this together, we conclude that there is a total adsorption barrier E_a^{ads}, which is composed of two components: one that is primarily influenced by molecular excitations E_0 and one which is primarily influenced by surface excitations E_a. Adsorption experiments probe reaction channels which exhibit barriers in both the surface and the molecule–surface coordinates. In desorption, however, it is primarily those reaction channels which have a barrier in the surface coordinates, but a low barrier in the molecule–surface coordinates that are open. The reason different reaction channels are open in adsorption compared to desorption will be discussed further in the next section.

C. Adsorption *contra* desorption

Hydrogen desorbed from Si does not appear to have traversed a large barrier to adsorption. Hence we are left to wonder why hydrogen sticks to Si with such a small probability if the adsorption barrier is small. Moreover, this apparent lack of an adsorption barrier presents a contradiction between adsorption and desorption experiments. In adsorption, the extremely low sticking coefficient of room temperature hydrogen on Si has generally been assumed to arise from a large energetic barrier to adsorption, which eventually could be overcome by large energies in the incoming beam. This assumption is partly corroborated by the S_{eff} vs T_n data reported here. In contrast, we find significant sticking only for elevated sample temperatures, and the fit to the data seems to suggest that even under these conditions sticking will saturate at $\leqslant 10^{-3}$ for $T_s = 630$ K.

We consider two possible explanations that may account for the inconsistency between adsorption and desorption experiments. Recent calculations from the Brenig group[45,46] have shown that translationally cool molecules can be observed in desorption even in the presence of an activation barrier to adsorption. This is the result of tunneling-dominated desorption and requires a rather thin barrier. Obviously tunneling would affect desorption in a different way than adsorption, since the adsorbed molecule can make an infinite number of attempts to tunnel through the barrier. Were tunneling to dominate desorption, one would expect there to be significant differences in the behavior of H_2 and D_2. In contrast to this expectation, the internal state distributions of H_2, HD, and D_2 are equivalent[22] and the rates of desorption for H_2 and D_2 exhibit no anomalous isotope effect.[2] Quantum effects must, therefore, either be negligible or counterbalancing. While we cannot as yet exclude this model completely, there is no experimental evidence aside from the cold translational distributions measured here which support it.

The second possible explanation is that the barrier to adsorption is not solely energetic in nature, but also, and in desorption effectively completely, entropic. In other words, only a very small portion of configuration space contains favorable adsorption trajectories, while all others experience high (>1 eV) barriers. As we have argued previously,[33] molecular orientation[47–49] and lattice impact parameters[49] certainly influence the effective adsorption barrier experienced by an incident molecule. While these two effects likely play a role in determining the sticking coefficient, it is difficult to imagine that they alone can account for a sticking coefficient of $<10^{-8}$, at room temperature or $\approx 10^{-5}$ at higher energies, especially since almost all configurations encounter a barrier of ≈ 1 eV, yet a fraction of the configurations traverse a rather marginal barrier. With reference to the H/Cu system, we note that the barrier is lower for special configurations compared to less favorable configurations, but it does not drop to zero. Thus we must search for another possible contributing factor for this restricted configuration space model.

We have proposed[33] that the third contribution arises from surface atom motion. This represents a component of the adsorption barrier which is sensitive to both energetics and entropic effects. Expressed differently, certain surface atom configurations result in an adsorption barrier that can be overcome by a low energy hydrogen molecule. Moving the surface atoms into these positions, however, requires some sort of phonon excitation and, therefore, increased surface temperature may lead to an increased probability of attaining these low barrier pathways.

Motion (reconstruction) of surface atoms is inherent to the chemisorption process of hydrogen on Si.[50–57] The barriers to adsorption and diffusion have been found in recent calculations[27–32,58–62] to be highly sensitive to the surface atom geometry. It is possible that in adsorption, the Si atoms

have to move into an appropriate geometry in order for an incident H_2 to complete successfully a dissociative trajectory and stay on the surface. In particular, it is known that the surface relaxes when the monohydride covers the surface. This effect has recently been directly measured for Si(100)-(2×1) by Rabalais and co-workers[17,63] using ion scattering techniques. They observe that the dimer bond, e.g., increases from 2.26±0.1 to 2.97±0.1 Å upon hydrogen adsorption. This expansion is much greater than that found in calculations for the H/Si system. For instance, calculations by Nachtigall, Jordan, and Janda[27] exhibit an expansion by 0.13 Å of the dimer from a clean-surface value of 2.32 Å to an adsorbate-covered value of 2.45 Å. This trend is typical of that observed in numerous other calculations.[28,31,59,64–66] Should the experimental results of Rabalais *et al.* be confirmed, this would demonstrate that significant improvements are required in the theoretical handling of the Si(100)-(2×1):H phase. We emphasize, however, that the value of 2.97 Å is extremely large compared to the bulk Si–Si bond length (2.35 Å)—a result which merits independent experimental confirmation.

Since Si atoms do not move rapidly compared to hydrogen, they very rarely get into a favorable configuration because the Si surface atoms do not have sufficient time to react under the influence of the impinging hydrogen molecule. Furthermore, an incident H_2 cannot force the Si atoms to assume the proper positions, because in an impulsive collision, the large mass mismatch prohibits an efficient transfer of energy to the lattice. As a consequence, the impinging H_2 experiences only those configurations which are present in the distribution arising from thermal vibrations of the lattice which may all be large barrier configurations. Therefore, adsorption experiments, such as the heated nozzle experiments presented here, yield results indicative of a barrier exceeding 1 eV.

In desorption, the system starts out with a relaxed lattice which should also have a lower Debye temperature than the clean surface. Calculations demonstrate that the vibrational amplitudes of the dimer atoms are sensitive to the strength of the coupling in the dimer bond.[67] Because adsorption destroys the Peierls-distortion induced stabilization of the clean dimer, hydrogen adsorption leads to greater thermal vibrational amplitudes of the dimer atoms. On the Si(111) surface, adsorbed H atoms weaken the bonding of Si adatoms to the underlying surface leading to the greater mobility of these atoms,[68,69] and a concomitantly greater vibrational freedom.

LEED and ion scattering data also indicate that lattice relaxation into a more bulklike configuration occurs.[51–57] Furthermore, Tromp *et al.*[54] employed ion scattering to determine that the Si(100)-(1×1):2H surface has a Debye temperature of 230 K. They were, however, unable to determine the clean surface Debye temperature, which is likely lower than the bulk value of 543 K; thus a direct comparison cannot be made. Wang *et al.*[70] have also reported that the Si(100)-(1×1):2H surface has a lower effective Debye temperature than the bulk. In this case, however, the difference is found to be much less pronounced than that reported by Tromp *et al.* Nonetheless, it seems safe to conclude that the hydrogen-covered surface will experience a greater thermal vibrational amplitude than the clean surface and that the hydrogen-covered surface is relaxed to a more bulklike configuration than the clean surface.

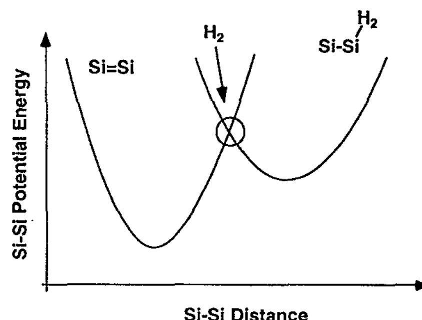

FIG. 5. A representation of Si dimer vibrational potentials before and after hydrogen adsorption within a Marcus theory framework. Because no energy exchange occurs between the scattering H_2 molecule and the Si dimer, the transition can only occur for those configurations for which the respective wave functions overlap (Franck–Condon transition).

Another point that underscores the importance of lattice effects is found, e.g., in the work of Verwoerd.[71] In these calculations, he determined that there is roughly an additional 0.5 eV of stabilization in the monohydride-covered surface that cannot simply be accounted for by the formation of the Si–H bonds. Additionally, Alerhand and Mele[72] demonstrated an intrinsic coupling between the phonons and electronic structure of Si surfaces. Such coupling provides a mechanism for producing an activation barrier that is not only sensitive to the surface geometry, but also to surface vibrational excitations.

In summary, this aspect is characterized as follows: Before adsorption, the two silicon atoms are tightly bound and their vibration is rather stiff. After the adsorption event, when the dimer bond is (partly) broken, not only is the equilibrium distance significantly larger, but also the vibrational mode is softer. Since the collision of the impinging hydrogen molecule with the dimer will hardly change the Si dimer vibrational motion, the transition between these two scenarios must be of Franck–Condon character (Fig. 5). Hence, it can only occur if the H_2 molecule strikes the dimer in a configuration which is, without change of position and momentum, also allowed for the dihydride intermediate state. Such a configuration corresponds to a large vibrational amplitude configuration due to the different Si–Si bond lengths prior to and after adsorption. The rate for adsorption is then limited by the probability of finding such configurations on the surface on the time scale of a collision. Since the collision time is short, this basically reduces to the probability that such configurations are populated in the thermal phonon spectrum. The population of such large vibrational amplitude configurations certainly increases with increasing temperature of the phonon distribution resulting in an apparent activation of the adsorption process with sample temperature.

Because of the relaxed geometry and greater thermal vibrational amplitude of the H-covered surface, a different and wider range of surface atom configurations is presented to the hydrogen atoms which attempt to recombine than can be

presented to an impinging hydrogen molecule. As a result, the recombining atoms can gain access to lower barrier pathways as they desorb from the surface than they could have seen in adsorption. Even though these low barrier configurations are improbable because they require large amplitude surface atom vibrations, simple argumentation based on the Arrhenius behavior of the desorption reaction shows that the smallest barrier processes will make the greatest contributions to the desorption rate. With this mechanism, we can explain the apparent contradictions observed in the adsorption/desorption results.

In summary, the restricted configuration space model relies on a surface structure dependent adsorption/desorption barrier that arises from the highly localized hydrogen–Si interaction. For certain configurations of the surface atoms and incident molecule, the barrier is low, i.e., holes appear in the adsorption barrier. In adsorption, these holes are rarely available because the corresponding surface atom configurations are far outside of the normal excursions of the surface atoms. Hence, only a small fraction of the flux can possibly stick. In desorption, where the lattice is relaxed and the surface Debye temperature may be much lower, the holes are more readily made available by surface excitations and the atoms have sufficient time to wait for these holes to open up. Therefore, desorption proceeds almost exclusively through these low activation energy pathways.

As a consequence, the two processes appear to follow two different potential energy hypersurfaces, calling into question the usual application of detailed balance. When examined more closely, however, we see that this *apparent* violation of detailed balance results from the high dimensionality of the adsorption/desorption process. The much different initial conditions of the two processes led to different probabilities at which low energy pathways are presented to the system. However, in both directions, trajectories can still follow the same pathways. These peculiarities are in stark contrast to the H/Cu system where trajectory studies have successfully modeled the adsorption/desorption process by considering desorption trajectories that started at a common transition state[73,74] or by performing calculations for adsorption alone.[75–78]

Even though the high dimensionality of the H/Si potential energy hypersurface is responsible for the observed behavior, it need not be necessary to invoke all of these dimensions to obtain an understanding of this system calculationally. Indeed, Brenig and co-workers[45,46] have succeeded in modeling our desorption results by invoking only two dimensions—one molecular and one corresponding to a surface oscillator. A crucial result of this work is that it shows how a "displaced" rather than a curved reaction path along the potential energy hypersurface can lead to vibrationally hot, but relatively translationally cool distributions in desorption. Therefore, the potential energy hypersurface of the H/Si system appears to have a decisively different topology than that of the H/Cu system.

The model of adsorption and desorption presented here predicts that surface vibrational excitation, i.e., the motions which change the configuration of the surface atoms, strongly affect the adsorption/desorption trajectories. Accordingly, we should expect that adsorption is enhanced by increased vibrational excitation of the surface. This prediction is borne out by the data in Fig. 4, in which we observe an increase in the effective sticking coefficient with increasing T_s. In the calculations of Brenig *et al.*, it is correspondingly found that the surface oscillator is left in an excited state after desorption. The apparent activation energy for this surface-excitation/surface-configuration-assisted adsorption pathway is ~0.31 eV. This pathway is also described by a relatively broad width of ~0.11 eV.

TABLE IV. E_d and A_d for H_2 desorption from Si(100) are tabulated with the corresponding values of the desorption rate constant k_d for T_s=800 K.

Footnote	E_d (eV)	A_d (s^{-1})	k_d (s^{-1}) T_s=800 K
a	1.95	2.2×10^{11}	0.112
a	2.17	2.2×10^{12}	0.048
b	2.51	5.5×10^{15}	0.790
b	2.86	6.5×10^{17}	0.610
c	2.48	2.0×10^{15}	0.475
d	2.48	2.0×10^{15}	0.475

[a]K. Sinniah, M. G. Sherman, L. B. Lewis, W. H. Weinberg, J. T. Yates, Jr., and K. C. Janda, J. Chem. Phys. **92**, 5700 (1990).
[b]M. L. Wise, B. G. Koehler, P. Gupta, P. A. Coon, and S. M. George, Surf. Sci. **258**, 166 (1991).
[c]U. Höfer, L. Li, and T. F. Heinz, Phys. Rev. B **45**, 9485 (1992).
[d]M. C. Flowers, N. B. H. Jonathan, Y. Liu, and A. Morris, J. Chem. Phys. **99**, 7038 (1993).

D. The role of defects

Models in which defects, which present virtually no barrier to adsorption, mediate adsorption/desorption have been proposed based on the results of cluster calculations. These models fall into two classes—diffusion-limited desorption to single atom defect sites[28,30–32] and dihydride desorption from single atom defects combined with defect migration.[29] Should adsorption take place only on very special defects, these would have to occupy $<10^{-5}$ and perhaps as little as 10^{-8} of all available sites in order to explain the low sticking coefficient. Equivalent sites in equivalent numbers would have to be present on both (100) and (111) surfaces in order to explain the low sticking coefficient and identical internal state distributions on both surfaces. The adatoms on the Si(111)-(7×7) structure bare a striking resemblance to what one might term single atoms defects. However, these are present in a concentration of 12/49 of a monolayer and, therefore, cannot function as barrierless adsorption sites.

First we note that support for a defect-mediated desorption mechanism has been sought[30] in the well-documented divergence of reported kinetic parameters for hydrogen desorption from Si. Let us remember that what is measured in a thermal desorption kinetics experiment is a pressure rise which is proportional to the absolute rate of the desorption reaction. The temperature and concentration (i.e., coverage) dependencies of this absolute rate are measured and then fitted to the appropriate rate equation. The *rate constant* is directly proportional to the actual measurement, while the *rate parameters* A_d and E_d are not because they are coupled.

Listed in Table IV are selected kinetic parameters for

H/Si(100) as well as the desorption rate constant k_d derived therefrom at a surface temperature approximately where the desorption rate has a maximum $T_s=800$ K. We note that even though A_d varies by six orders of magnitude, the *rate constants* deviate by only a factor of 16. In all likelihood, the extreme values measured in footnote a are erroneous either due to some undetected systematic error or due to a fitting error caused by a local minimum in the analysis. The values of footnotes b, c, and d also agree very well with desorption data from Si(111) (see footnote c and Ref. 4), which further lends credence to these values. Thus little support for a defect-mediated desorption mechanism can be found in these data.

When considering defect-mediated models, not only the results presented here, but also the kinetics of adsorption and desorption from both the Si(100) and Si(111) surfaces must be considered as well as the results of the quantum-state resolved desorption experiments of Kolasinski, Shane, and Zare.[22–25] The main criteria which have to be satisfied are the following: (i) nearly equivalent transitions states, with respect to the forces applied to the newly forming hydrogen molecule, are reached during desorption from the monohydride phases on Si(100) and Si(111) as well as for the mixed mono/dihydride phase on Si(100); (ii) the desorption kinetics from Si(100) are *nominally* first order, however, deviations from first-order kinetics are observed which suggest the importance of pairing before desorption occurs; (iii) the desorption kinetics from Si(111) are *nominally* second order, however, deviations from second-order kinetics are observed, which suggest the importance of desorption from two independent sites, e.g., from the rest-atom and adatom sites; (iv) the rate constants for monohydride desorption on both surfaces are nearly identical; (v) the saturation value of the sticking coefficient cannot be greater than the concentration of the defects which present no barrier to adsorption; and (vi) adsorption is activated by 0.31 eV in the surface coordinates.

Point (i) can be satisfied by a defect-mediated mechanism under the assumption that a dihydride species is formed on both Si(100) and Si(111). The localized interactions in the H/Si system could reasonably make the immediate vicinity of an adsorbed SiH_2 species irrelevant to the forces on the departing H_2 molecule.

If a diffusion-limited desorption mechanism were active on Si(100), but not on Si(111), we are left with the task of trying to explain the coincidence of the nearly identical rate constants for desorption on these two surface and why the diffusion behavior is dramatically different on the two surfaces. Furthermore, within the single-atom-defect models, there is no good explanation for the deviations from first-order desorption kinetics observed on Si(100). If the rate-limiting step is desorption from dihydride units adsorbed on defect sites on Si(100), but dihydride formation on Si(111), we again are left with perplexing tasks of explaining the kinetic deviations on Si(100) and the coincidence of the nearly identical desorption rate constants. Moreover, the adatoms sites on the Si(111)-(7×7) surface represent natural "single-atom defects" on this surface, yet they do not suffice for the facile adsorption of molecular hydrogen. Thus defect-mediated mechanisms do not appear to be consistent with points (ii)–(iv). Note also that we observed no dependence of $\langle E_{\text{trans}} \rangle$ on coverage. This suggests that the dynamics do not change as a function of coverage as would be expected in a defect-mediated process.

Concerning points (v) and (vi), in this work we have determined that the value of the sticking coefficient is T_s and T_n dependent. The saturation value of the sticking coefficient is of the order of 1×10^{-3} as $T_n\rightarrow\infty$ at $T_s=630$ K, but is of the order unity as $T_s\rightarrow\infty$. Therefore the sites responsible for sticking must have a concentration $\geqslant 1\times10^{-3}$ at 630 K and near unit concentration as T_s becomes large. One could interpret this result as suggesting that the concentration of the "defects" active in the desorption process increases with increasing T_s. However, it is also the case that the mean square displacements of normal Si surface atoms increases with T_s and, therefore, the model proposed by us also predicts that the saturation value of the sticking coefficient increases with increasing T_s. We suggest, therefore, that the defects alluded to in the calculations of Wu *et al.*,[28,30] Jing and Whitten,[31,32] and Nachtigall *et al.*[29] are actually normal Si surface atoms which are at positions different from their equilibrium position, but within the range of their normal thermal oscillations at the given surface temperature. The activation energy for the "formation" of these defects can be identified with 0.31 eV measured here. Our results emphasize that surface relaxations, as well as the lattice dynamics during adsorption/desorption, must be properly treated in order to obtain a complete theoretical description of the adsorption and desorption dynamics.

V. CONCLUSION

Direct evidence of activated adsorption of hydrogen has been presented. By increasing the surface temperature, the sticking coefficient increases. An increase in the sticking coefficient can also be produced by increasing the translational and vibrational energy contents of the incident hydrogen molecule. We hasten to point out that the absolute values of the sticking coefficient and the barrier heights derived from the fits possess a large susceptibility to error. Nonetheless, the data clearly demonstrate that there is a significant barrier to adsorption for incident molecules and that the surface temperature does play a significant role in determining the sticking coefficient for hydrogen adsorption on Si.

The nominally first-order kinetics observed for Si(100) results from the influence of hydrogen-atom pairing on dimer units. The nominally second-order desorption kinetics for Si(111) result from the influence of (at least) two active sites in the desorption process. In both cases, it is the formation of the dihydride species which is the rate limiting step; otherwise, the kinetic behavior cannot adequately be explained. Neither a diffusion-limited desorption mechanism nor the influence of defects is required for a consistent interpretation of the adsorption and desorption data.

We argue that a proper treatment of surface atom configurations and motions is essential for understanding the adsorption and desorption mechanisms. In reflecting on our proposed reaction mechanism, we note that it bears a striking resemblance to essential aspects of the Marcus theory of

electron transfer.[79] We are currently investigating the possibility of applying this theoretical framework to hydrogen desorption from Si.

The apparent breakdown of detailed balance is essentially a matter of the different time scales for the interactions in adsorption and desorption. In desorption, the H atoms can wait until surface excitations present them with a low barrier desorption pathway. The time scale of the molecule–surface interaction for the case of adsorption, however, is the duration of a molecule–surface collision. During this period, the surface does not have sufficient time to change its configuration. Thus, low barrier pathways are only presented to the incident molecule if the surface has already attained the appropriate configuration prior to the collision. For the clean, room temperature surface exposed to a Boltzmann distribution of hydrogen gas, this is a very unlikely event. It is clear from the proposed reaction mechanism that the adsorption/desorption dynamics of H/Si are decisively different from those of H/Cu.

ACKNOWLEDGMENTS

Professor Wilhelm Brenig and Professor Emily Carter are thanked for numerous discussions and for providing us with results prior to publication. Professor Ken Jordan also provided us with results prior to publication. We acknowledge with pleasure the continual support of Professor Gerhard Ertl and the Alexander von Humboldt Stiftung for providing a postdoctoral fellowship for K.W.K.

[1] K. Sinniah, M. G. Sherman, L. B. Lewis, W. H. Weinberg, J. T. Yates, Jr., and K. C. Janda, Phys. Rev. Lett. **62**, 567 (1989).
[2] K. Sinniah, M. G. Sherman, L. B. Lewis, W. H. Weinberg, J. T. Yates, Jr., and K. C. Janda, J. Chem. Phys. **92**, 5700 (1990).
[3] M. L. Wise, B. G. Koehler, P. Gupta, P. A. Coon, and S. M. George, Surf. Sci. **258**, 166 (1991).
[4] G. A. Reider, U. Höfer, and T. F. Heinz, J. Chem. Phys. **94**, 4080 (1991).
[5] U. Höfer, L. Li, and T. F. Heinz, Phys. Rev. B **45**, 9485 (1992).
[6] J. J. Boland, Phys. Rev. Lett. **67**, 1539 (1991).
[7] P. C. Weakliem, G. W. Smith, and E. A. Carter, Surf. Sci. **232**, L219 (1990).
[8] P. C. Weakliem and E. A. Carter, J. Chem. Phys. **96**, 3240 (1992).
[9] F. H. Stillinger, Phys. Rev. B **46**, 9590 (1992).
[10] G. K. Wertheim, D. M. Riffe, J. E. Rowe, and P. H. Citrin, Phys. Rev. Lett. **67**, 120 (1991).
[11] R. Wiesendanger, D. Bürgler, G. Tarrach, H.-J. Güntherodt, I. V. Shvets, and J. M. D. Coey, Surf. Sci. **274**, 93 (1992).
[12] Z. Jing and J. L. Whitten, Surf. Sci. **274**, 106 (1992).
[13] J. Dabrowski and M. Scheffler, Appl. Surf. Sci. **56–58**, 15 (1992).
[14] R. A. Wolkow, Phys. Rev. Lett. **68**, 2636 (1992).
[15] A. I. Shkrebtii and R. Del Sole, Phys. Rev. Lett. **70**, 2645 (1993).
[16] A. García and J. E. Northrup, Phys. Rev. B **48**, 17350 (1993).
[17] Y. Wang, M. Shi, and J. W. Rabalais, Phys. Rev. B **48**, 1678 (1993).
[18] K. Cho and J. D. Joannopoulos, Phys. Rev. Lett. **71**, 1387 (1993).
[19] M. P. D'Evelyn, Y. L. Yang, and L. F. Sutcu, J. Chem. Phys. **96**, 852 (1992).
[20] M. P. D'Evelyn, S. M. Cohen, E. Rouchouze, and Y. L. Yang, J. Chem. Phys. **98**, 3560 (1993).
[21] Y. L. Yang and M. P. D'Evelyn, J. Vac. Sci. Technol. A **11**, 2200 (1993).
[22] K. W. Kolasinski, S. F. Shane, and R. N. Zare, J. Chem. Phys. **96**, 3995 (1992).
[23] S. F. Shane, K. W. Kolasinski, and R. N. Zare, J. Vac. Sci. Technol. A **10**, 2287 (1992).
[24] S. F. Shane, K. W. Kolasinski, and R. N. Zare, J. Chem. Phys. **97**, 3704 (1992).
[25] S. F. Shane, K. W. Kolasinski, and R. N. Zare, J. Chem. Phys. **97**, 1520 (1992).
[26] Y.-S. Park, J.-Y. Kim, and J. Lee, J. Chem. Phys. **98**, 757 (1993).
[27] P. Nachtigall, K. D. Jordan, and K. C. Janda, J. Chem. Phys. **95**, 8652 (1991).
[28] C. J. Wu, I. V. Ionova, and E. A. Carter, Surf. Sci. **295**, 64 (1993).
[29] P. Nachtigall, K. D. Jordan, and C. Sosa, J. Chem. Phys. (to be published).
[30] C. J. Wu, I. V. Ionova, and E. A. Carter, Phys. Rev. B (to be published).
[31] Z. Jing and J. L. Whitten, J. Chem. Phys. **98**, 7466 (1993).
[32] Z. Jing, G. Lucovsky, and J. L. Whitten, Surf. Sci. **296**, L33 (1993).
[33] K. W. Kolasinski, W. Nessler, A. de Meijere, and E. Hasselbrink, Phys. Rev. Lett. **72**, 1356 (1994).
[34] J. A. Barker and D. J. Auerbach, Surf. Sci. Rep. **4**, 1 (1985).
[35] G. Comsa and R. David, Surf. Sci. Rep. **5**, 145 (1985).
[36] H. A. Michelsen and D. J. Auerbach, J. Chem. Phys. **94**, 7502 (1991).
[37] E. P. Wenaas, J. Chem. Phys. **54**, 376 (1971).
[38] M. Liehr, C. M. Greenlief, M. Offenberg, and S. R. Kasi, J. Vac. Sci. Technol. A **8**, 2960 (1990).
[39] E. Hasselbrink, S. Jakubith, S. Nettesheim, M. Wolf, A. Cassuto, and G. Ertl, J. Chem. Phys. **92**, 3154 (1990).
[40] W. E. Lamb, Jr. and R. C. Retherford, Phys. Rev. **79**, 549 (1950).
[41] B. G. Koehler and S. M. George, Surf. Sci. **248**, 158 (1991).
[42] H. A. Michelsen, C. T. Rettner, D. J. Auerbach, and R. N. Zare, J. Chem. Phys. **98**, 8294 (1993).
[43] C. T. Rettner, H. A. Michelsen, and D. J. Auerbach, Faraday Discuss. Chem. Soc. (to be published).
[44] M. C. Flowers, N. B. H. Jonathan, Y. Liu, and A. Morris, J. Chem. Phys. **99**, 7038 (1993).
[45] W. Brenig, T. Brunner, A. Gross, and R. Russ, Z. Phys. B **93**, 91 (1993).
[46] W. Brenig, A. Gross, and R. Russ, Phys. Rev. Lett. (to be published).
[47] B. I. Lundqvist, O. Gunnarsson, H. Hjelmberg, and J. K. Nørskov, Surf. Sci. **89**, 196 (1979).
[48] S. Holloway, J. Phys. Condensed Matter **3**, S43 (1991).
[49] P. J. Feibelman, Phys. Rev. Lett. **67**, 461 (1991).
[50] J. J. Boland, Adv. Phys. **42**, 129 (1993).
[51] R. J. Culberson, L. C. Feldman, and P. J. Silverman, J. Vac. Sci. Technol. **20**, 868 (1982).
[52] S. Ciraci, R. Butz, E. M. Oellig, and H. Wagner, Phys. Rev. B **30**, 711 (1984).
[53] S. Maruno, H. Iwasaki, K. Horioka, S.-T. Li, and S. Nakamura, Phys. Rev. B **27**, 4110 (1983).
[54] R. M. Tromp, R. G. Smeenk, and F. W. Saris, Surf. Sci. **104**, 13 (1981).
[55] R. M. Tromp, J. Vac. Sci. Technol. A **1**, 1047 (1983).
[56] E. G. McRae and C. W. Caldwell, Phys. Rev. Lett. **46**, 1632 (1981).
[57] S. J. White, D. P. Woodruff, B. W. Holland, and R. S. Zimmer, Surf. Sci. **74**, 34 (1978).
[58] C. J. Wu and E. A. Carter, Chem. Phys. Lett. **185**, 172 (1991).
[59] C. J. Wu and E. A. Carter, Phys. Rev. B **46**, 4651 (1992).
[60] A. Vittadini, A. Selloni, and M. Casarin, Surf. Sci. **289**, L625 (1993).
[61] B. R. Wu and C. Cheng, J. Phys. Condensed Matter **6**, 1113 (1994).
[62] Z. Jing and J. L. Whitten, Phys. Rev. B **48**, 17296 (1993).
[63] M. Shi, Y. Wang, and J. W. Rabalais, Phys. Rev. B **48**, 1689 (1993).
[64] X. M. Zheng and P. V. Smith, Surf. Sci. **279**, 127 (1992).
[65] B. I. Craig and P. V. Smith, Surf. Sci. **226**, L55 (1990).
[66] B. I. Craig and P. V. Smith, Phys. Status Solidi B **170**, 518 (1991).
[67] K. Ohkuma and K. Nakamura, J. Phys. C **12**, L835 (1979).
[68] J. J. Boland, J. Phys. Chem. **95**, 1521 (1991).
[69] K. Mortensen, D. M. Chen, P. J. Bedrossian, J. A. Golovchenko, and F. Besenbacher, Phys. Rev. B **43**, 1816 (1991).
[70] Y. Wang, S. V. Teplov, O. S. Zaporozchenko, V. Bykov, and J. W. Rabalais, Surf. Sci. **296**, 213 (1993).
[71] W. S. Verwoerd, Surf. Sci. **108**, 153 (1981).
[72] O. L. Alerhand and E. J. Mele, Phys. Rev. B **35**, 5533 (1987).
[73] J. Harris, Appl. Phys. A **47**, 63 (1988).
[74] J. Harris, Surf. Sci. **221**, 335 (1989).
[75] G. R. Darling and S. Holloway, J. Chem. Phys. **97**, 5182 (1992).
[76] G. R. Darling and S. Hollway, Surf. Sci. **268**, L305 (1992).
[77] D. Halstead and S. Holloway, J. Chem. Phys. **93**, 2859 (1990).
[78] S. Holloway and X. Y. Chang, Faraday Discuss. Chem. Soc. **91**, 425 (1991).
[79] R. A. Marcus and N. Sutin, Biochim. Biophys. Acta **811**, 265 (1985).